ResBeat: Resilient Breathing Beats Monitoring with Realtime Bimodal CSI data

Xuyu Wang, Chao Yang, and Shiwen Mao
Department of Electrical and Computer Engineering, Auburn University, Auburn, AL 36849-5201, USA
Email: {xzw0029, czy0017}@auburn.edu, smao@ieee.org

***Abstract*—Vital signs, such as breathing rate, can provide useful information for personal healthcare. In this paper, we present ResBeat, a commodity 5GHz WiFi based system to exploit bimodal channel state information (CSI), including amplitude and phase difference, for realtime, long-term, and contact-free breathing monitoring. We first present an analysis of breathing signal anomaly based on bimodal CSI data. We then describe the data preprocessing, adaptive signal selection, and breathing signal monitoring modules of ResBeat, and employ peak detection to estimate breathing rates. We conduct extensive experiments under three different environments, where superior performance over two alternative methods is validated.**

***Index Terms*—Vital sign monitoring; breathing rate monitoring; channel state information (CSI); bimodal CSI data; WiFi.**

I. Introduction

Vital signs can provide useful clues to many diseases such as heart disease, lung disorder, and diabetes, which cost considerable expenses for treatment [1]. For example, monitoring breathing signals can help a patient to detect sleep disorders or anomalies, and prevent sudden infant death syndrome (SIDS) for sleeping infants [2]. To provide effective cure for such diseases, daily measurements of human respiratory rate are becoming increasingly important. However, a conventional breathing rate measurement method is to count manually with a stethoscope or a specific device such as a capnography [3], which are both inconvenient to use and discomfort to patients. Furthermore, when a patient is being monitored, he or she may intentionally reduce the breathing rate or breath more smoothly, leading to inaccurate results. Effective solutions are in great demand for realtime, long-term, and contact-free breathing signal monitoring [4], [5].

To this end, several wireless vital signal monitoring systems have been proposed in the literature, which mainly leverage RF signals to detect the chest fluctuation caused by respiration. For example, Vital-Radio can measure breathing and heart rates for multiple people simultaneously using a frequency modulated continuous wave (FMCW) radar [6]. Another system, mmVital, detects the received signal strength (RSS) of 60 GHz millimeter wave (mmWave) signals to estimate respiratory rate and heart rate [7]. Both systems require a wide spectrum to operate on as well as specially designed hardware. Moreover, some other techniques, such as Doppler radar [8] and ultra-wideband radar [9], can also monitor vital signs, but also requiring dedicated hardware at high frequency with high costs. Finally, Ubibreathe is developed with off-the-shelf WiFi devices, and uses RSS at a WiFi device held on a person's chest for breathing detection [10]. It requires the person to be situated on the line-of-sight (LOS) path between the device and the WiFi access point.

Unlike RSS, channel state information (CSI) provides fine-grained physical layer (PHY) information, which can be extracted by open-source device drivers such as Intel WiFi Link 5300 NIC [11] and Atheros AR9580 chipset [12]. It can reveal the channel characteristics experienced by the received signal, including multipath effect and shadow fading. Moreover, CSI data is a more stable representation of channel characteristics, including amplitude and phase information of subcarrier-level measurements in the orthogonal frequency division multiplexing (OFDM) system. Recently, CSI amplitude based method is proposed for monitoring breathing and heart beats when a person is sleeping [13]. In addition, our recent works PhaseBeat [14] and TensorBeat [15] leverage CSI phase difference data to monitor a single person's vital signals and multiple persons' breathing signals, respectively. However, these works are not effective in detecting the weak breathing signals at some special locations [16], which motivates us to use bimodal CSI data for resilient breathing monitoring.

In this paper, we employ CSI amplitude and phase difference bimodal data to detect and monitor breathing beats with commodity 5GHz WiFi devices. For indoor environments under small-scale fading, we consider the chest reflected signal as a *dynamic component*, while lumping the line-of-sight (LOS) and all other multipath signals together as a *static component*. We model the amplitude and phase response of the CSI subcarriers with the dynamic and static component approach, and prove that CSI amplitude and phase information carry the breathing information with the same rate. Moreover, we present an analysis of breathing signal anomaly with CSI amplitude and phase information, and show that the breathing signals can be weak at some monitoring locations. Thus, we propose to use bimodal CSI data for resilient breathing monitoring, due to the fact that CSI amplitude and phase difference data in consecutively received packets are stable, and they are complementary to each other with respect to mitigating the anomalous breathing signals at some bad locations. The bimodal data is also robust to environment interferences and body movements for breathing signal monitoring.

We present the design of ResBeat, i.e., **Res**ilient realtime breathing **Beat** monitoring with bimodal CSI amplitude and phase difference data with commodity WiFi devices. The

ResBeat system consists of data preprocessing, adaptive signal selection, and breathing signal monitoring modules. For data preprocessing, we calibrate CSI data with an *exponentially weighted moving average* (EWMA) method to extract the static, or environment, component and the dynamic, or breathing, component. For adaptive signal selection, we propose a signal selection algorithm based on signal energy detection and movement detection, to select the most sensitive signal group, which can successfully mitigate the effect of anomalous breathing signals. Finally, the peak detection method is used to estimate breathing rates in realtime CSI data.

We implement ResBeat with commodity 5GHz WiFi devices and evaluate its performance with four persons over three months in different indoor environments, such as a computer laboratory, a through-wall scenario, and a long corridor. The results validate that the ResBeat system can achieve high estimation accuracy of breathing rate with a median error of 0.25 bpm (beats per minute), and has a higher success rate of 90% for breathing rate detection at different locations.

In the rest of this paper, the preliminaries and the breathing signal anomaly analysis are presented in Section II. We discuss the ResBeat system design in Section III and validate its performance in Section IV. Section V summarizes this paper.

II. Breathing Signal Anomaly Analysis

A. Channel State Information Preliminaries

Many wireless network standards (such as WiFi, LTE, WiMAX, and DVB) employ OFDM for data transmission, to deal with frequency selective channels and achieve high data rates. In OFDM, the spectrum is divided into multiple orthogonal subcarriers to form narrowband channels. Wireless data can be transmitted with different modulation and coding schemes (MCS) to mitigate channel fading and large delay spreads, while cyclic redundancy is used to reduce the complexity of FFT processing at the receiver. Open-source devices drivers are available for extracting data from several off-the-shelf NICs, e.g., Intel WiFi Link 5300 NIC [11] and the Atheros AR9580 chipset [12]. The Intel 5300 NIC is used in ResBeat to obtain CSI data, which reports 30 out of the 56 subcarriers at the WiFi receiver for a 20 MHz or 40 MHz channel.

The channel frequency response of subcarrier i, H_i, can be written as

$$\mathrm{H}_i = |\mathrm{H}_i| \exp\left(j\angle\mathrm{H}_i\right), \ \forall\, i, \tag{1}$$

where $|\mathrm{H}_i|$ and $\angle\mathrm{H}_i$ are the amplitude response and phase response of subcarrier i, respectively.

B. Breathing Signal Anomaly Analysis

We consider indoor environments with NLOS components [17], [18], where the chest reflected signal is regarded as the *dynamic component*, and the sum of the LOS and all other mutipath signals is regarded as a *static component*. Thus, the channel frequency response of subcarrier i, denoted by H_i, can be written as

$$\begin{aligned}\mathrm{H}_i &= \sum_{k=0,k\neq d}^{K} r_k \cdot e^{-j2\pi f_i \tau_k} + r_d \cdot e^{-j2\pi f_i \tau_d} = \mathrm{H}_i^s + \mathrm{H}_i^d \\ &= |\mathrm{H}_i^s| \exp\left(j\angle\mathrm{H}_i^s\right) + |\mathrm{H}_i^d| \exp\left(j\angle\mathrm{H}_i^d\right),\end{aligned} \tag{2}$$

where K is the number of multipaths, r_k and τ_k are the attenuation and propagation delay of the k_{th} path, respectively; $\mathrm{H}_i^s = \sum_{k=0,k\neq d}^{K} r_k \cdot e^{-j2\pi f_i \tau_k}$ is the static component and $\mathrm{H}_i^d = r_d \cdot e^{-j2\pi f_i \tau_d}$ is the dynamic component, $|\mathrm{H}_i^s|$ and $\angle\mathrm{H}_i^s$ are the amplitude and phase of H_i^s, respectively, and $|\mathrm{H}_i^d|$ and $\angle\mathrm{H}_i^d$ are the amplitude and phase of H_i^d, respectively.

The amplitude response of subcarrier i can be computed as

$$|\mathrm{H}_i| = \sqrt{|\mathrm{H}_i^s|^2 + |\mathrm{H}_i^d|^2 + 2|\mathrm{H}_i^s||\mathrm{H}_i^d| \cos\left(\angle\mathrm{H}_i^s - \angle\mathrm{H}_i^d\right)}. \tag{3}$$

In (3), the amplitude and phase of the static component H_i^s are regarded as constants, and the amplitude of the dynamic component H_i^d is also assumed to be constant. Moreover, the phase of the dynamic component H_i^d can be modeled as $\angle\mathrm{H}_i^d = 2\pi L/\lambda_i$, where λ_i is the wavelength of subcarrier i and L is the distance of the dynamic path going through the chest. Note that the phase of the dynamic component H_i^d is periodic because the dynamic path distance L is periodic due to chest movements (i.e., it gets slightly longer when exhaling and shorter when inhaling). Thus, the amplitude response of subcarrier i, $|\mathrm{H}_i|$, is also periodic. In most cases, the CSI amplitude can effectively capture the breathing signal. However, at some monitoring locations, when the phase difference between the static component H_i^s and the dynamic component H_i^d is nearly zero, the variations of the CSI amplitude will be small, leading to high monitoring errors.

This is illustrated in Fig 1, where the geometric relationship of the static and dynamic components is presented. The dynamic components are $\overrightarrow{SD}_i$, $i = 1, 2, 3, 4$, and the static component is $\overrightarrow{OS}$. We can see that when the dynamic vector oscillates between $\overrightarrow{SD}_1$ and $\overrightarrow{SD}_2$, the CSI amplitude varies between $|\overrightarrow{OD}_1|$ and $|\overrightarrow{OD}_2|$, with very small variations. Such small variations in the CSI amplitude leads to a weak breathing signal and high detection error.

On the other hand, let's consider the phase response of subcarrier i, $\angle\mathrm{H}_i$, which can be written as [14]

$$\angle\mathrm{H}_i = \angle\mathrm{H}_i^s - \arctan\left\{\frac{|\mathrm{H}_i^d|\cdot\sin(\angle\mathrm{H}_i^s - \angle\mathrm{H}_i^d)}{|\mathrm{H}_i^d|\cdot\cos(\angle\mathrm{H}_i^s - \angle\mathrm{H}_i^d) + |\mathrm{H}_i^s|}\right\}. \tag{4}$$

Note that the phase response of subcarrier i is also periodic, which can be used to detect breathing rate. However, there are also some cases where the phase information is not effective for monitoring breathing signals. As shown in Fig 1, when the dynamic vector oscillates between $\overrightarrow{SD}_3$ and $\overrightarrow{SD}_4$, the phase value changes slightly between $\angle\overrightarrow{OD}_3$ and $\angle\overrightarrow{OD}_4$. Such negligible variations in phase value makes it hard to detect the breathing rate with phase information in this situation.

Fortunately, we can see that in the first example, when the variation in CSI amplitude is small, the change in CSI phase is between $\angle\overrightarrow{OD}_1$ and $\angle\overrightarrow{OD}_2$, which is quite large. On the other

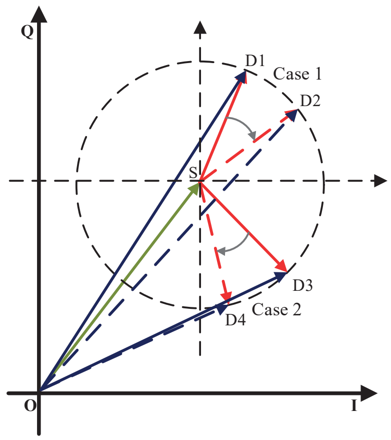

Fig. 1. The geometric relationship of the static and dynamic components for breathing signal anomaly analysis.

hand, in the second example when the variation in CSI phase is small, the change in CSI amplitude is between $|\overrightarrow{OD}_3|$ and $|\overrightarrow{OD}_4|$, which is also quite large. This observation motivates us to leverage bimodal CSI data, including CSI amplitude and phase, for resilient breathing monitoring.

Furthermore, it has been shown that the measured CSI phase data is not stable, due to the randomness in the RF chain, such as packet boundary detection (PBD), the sampling frequency offset (SFO), and central frequency offset (CFO) [14], [15]. We thus use the measured *phase difference* data instead in ResBeat, which is given by

$$\Delta\angle\widehat{H}_i = \Delta\angle \mathrm{H}_i + \Delta\beta + \Delta Z, \tag{5}$$

where $\Delta\angle\mathrm{H}_i$ is the true phase difference of subcarrier i, $\Delta\beta$ is the unknown difference in phase offsets, which is a constant [19], and ΔZ is the noise difference. Obviously, $\Delta\angle\widehat{H}_i$ is a stable signal for different received packets, since the randomness due to PBD, SFO, and CFO are canceled. Thus, we use bimodal CSI amplitude and phase difference data in ResBeat to deal with anomalous breathing signals.

III. The ResBeat System

A. ResBeat System Architecture

The main idea of the proposed ResBeat system is to monitor breathing signals using realtime bimodal CSI data from 5GHz WiFi devices. We propose an adaptive signal selection method to select the most sensitive CSI data, i.e., amplitude or phase difference, to mitigate the anomalous breathing signals, as shown in Fig. 1. The ResBeat system can effectively exploit realtime bimodal CSI data to monitor breathing beats for three reasons. First, CSI amplitude and phase difference data are quite stable for consecutive packets in a stationary environment, both of which can effectively capture the breathing beats. Second, CSI amplitude and phase difference data are complementary to each other with respect to their resilience to the two anomalous cases shown in Fig. 1. Using the bimodal data can effectively deal with anomalous breathing signals. Third, ResBeat is robust to environment interference and body movements by using the bimodal CSI data.

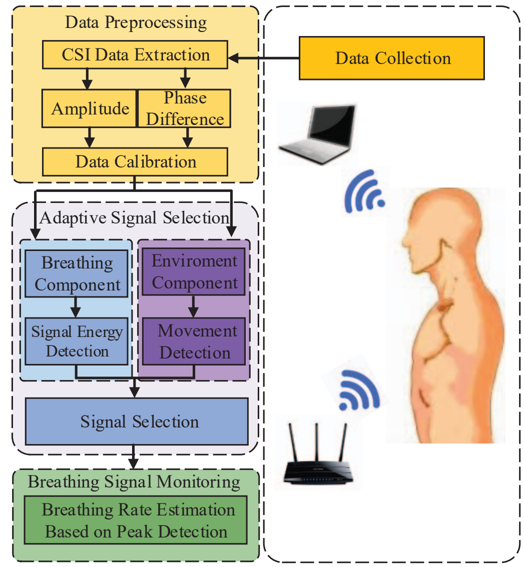

Fig. 2. The ResBeat system architecture.

Fig. 2 presents the ResBeat system architecture, which consists of three main modules: Data Preprocessing, Adaptive Signal Selection, and Breathing Signal Monitoring. We describe the design of these three modules in the following.

B. Data Preprocessing

1) CSI Data Extraction: We collect 90 CSI values for every received packet from the three antennas of the IEEE 802.11n NIC, each of which provide CSI values from 30 subcarriers (i.e., 90 CSI amplitude and phase values). We employ three groups of CSI amplitude values from antennas 1, 2, and 3, respectively. We also use (5) to obtain three groups of CSI phase difference values from antennas 1 and 2, antennas 2 and 3, and antennas 3 and 1, respectively. Each group includes 30 values, which will be processed in the next step.

2) Data Calibration: Data calibration is to partition the original CSI amplitude and phase difference data into the static component (or, the *environment component*) and the dynamic component (or, the *breathing component*). The environment component can represent the change of wireless channel from the surrounding environment such as reflection from walls, desks and stationary body of a person. On the other hand, the breathing component can represent the change of wireless signal due to chest movements when inhaling and exhaling.

In ResBeat, the environment component can be extracted using the EWMA method, which is based on a first-order autoregressive model [20]. Let Y_t be the realtime CSI data (i.e., CSI amplitude or phase difference), and M_t be its local mean. We have

$$M_t = \rho \cdot Y_t + (1-\rho)\cdot M_{t-1}, \text{ for } t = 1, 2, ..., n, \tag{6}$$

where ρ is a parameter that determines the relative weights of the recent sample value and historical values, and n is the

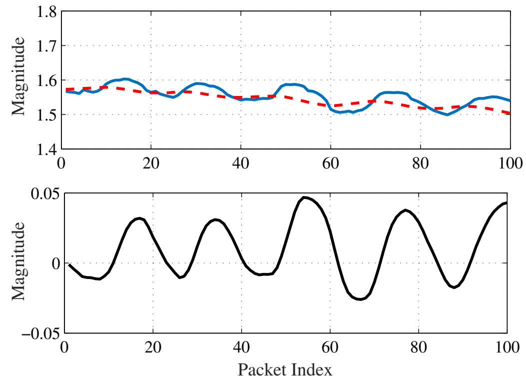

Fig. 3. Data calibration results.

number of observed samples. In our experiments, we set $\rho = 0.1$ to obtain the environment component.

We propose the EWMA method for extracting the environment component for three reasons. First, the EWMA method does not require a large data buffer and is suitable for realtime breathing monitoring. Second, as the moving average (MA) method, the EWMA method can effectively extract the outline of realtime data, from which the breathing signal can be filtered. Last but not least, compared with MA, EWMA is more sensitive to the more recent sample data. When the body moves, EWMA will capture a large change in M_t and thus can have a more rapid response, which is beneficial for detecting environmental changes.

After obtaining the environment component, we first apply the MA method to the original CSI data to remove high frequency noises, where the window size is set to 3. Then, the breathing component can be extracted by subtracting the environment component from the denoised CSI data. Fig. 3 illustrates calibration of the original phase difference. We can see in the top plot that the original phase difference values, for subcarrier 5 between antennas 1 and 2, have a direct current (DC) component as well as high frequency noises. Applying the EWMA method, we can obtain the environment component, which is the outline of the original phase difference. Then, the breathing component can be extracted by de-noising the CSI phase difference data and removing the environment component, which exhibits a sinusoidal-like periodicity over the received packets with low noise (see the bottom plot).

C. Adaptive Signal Selection

In this module, we design signal energy detection and movement detection to select the most sensitive signal group from the three CSI amplitude groups and the three CSI phase difference groups. As shown in Fig. 1, these groups have different levels of sensitivity to the same measured CSI data.

1) Signal Energy Detection: We use the energy value of the breathing component as a measure of the sensitivity of CSI amplitude and phase difference information. Recall that each CSI data group consists of 30 values from every received packet (e.g., either being CSI amplitude or phase difference). We use a window size of 20 to compute the local energy of each CSI data group j, denoted as $E_j(k)$, as

$$E_j(k) = \sum_{i=1}^{i=30} \sum_{t=k-19}^{t=k} \left| Y_{ij}^d(t) \right|^2, \tag{7}$$

where k is the current data index, and $Y_{ij}^d(t)$ is the normalized breathing component data in CSI data group j from subcarrier i at time t. Compared with other more advanced methods (e.g., FFT), the signal energy detection method can not only leverage smaller data values to measure the sensitivity of CSI data, but also be suitable for realtime measurement. The signal energy values of the CSI groups are then used for signal selection.

2) Movement Detection: In this module, we make use of the environment component in the phase difference data to detect body movement. We choose phase difference data because it has a fixed range between $-\pi$ and π, while CSI amplitude data has a variable range. We first compute the average of the environment components of all the phase difference data over the 30 subcarriers, which can be used to detect body movement by comparing with adjacent average values. In fact, the phase difference data can increase or decrease due to body movement. Thus, a body movement is detected if the current average value is lower than 0.95 times or larger than 1.05 times of the previous average value.

Furthermore, we find that small movements of the body or movements from nearby persons may also cause large changes in the average of the environment component. We propose a counting method to deal with such small body movements and environmental interference. The counting method is designed as follows. First, the count is initialized to 0. Then, the count will be increased by 1 when the current average value of phase difference data is lower than 0.95 times or larger than 1.05 times of the last average value. However, once the above condition is violated, the count will be reset to 0. A movement is detected if and only if the count reaches 10. In ResBeat, we implement the counting method that uses the three CSI phase difference data groups for movement detection. If a movement is detected in one of the CSI phase difference data groups, ResBeat will execute the following signal selection algorithm.

3) Signal Selection: This module is to select the most sensitive group from the six bimodal CSI data groups, for accurate breathing signal monitoring. The procedure is presented in Algorithm 1. The input parameters include the movement detection flag (mov_flag) and the local energy of each signal group (E_1, E_2, ..., E_6) computed as in (7). The output is the index of the most sensitive CSI data group.

In the beginning, we use 30 phase difference data from antennas 1 and 2 to implement the signal selection no matter whether a movement is detected or not. After the initialization, we use the above movement detection module based on the counting method to determine whether the environment has a large change. When a movement is detected, we run the signal selection again. First, the system will wait for 2 seconds so that the environment components based on EWMA can return to stable values (recovers from the movement). Then, the system sorts the signal groups (i.e., 1–6) in descending order of the

Algorithm 1: Signal Selection Algorithm

Input: movement detection flag (mov_flag) and the local energy of each data group (E_1, E_2, ..., E_6);
Output: index of the most sensitive data group;
Set $initialize\_flag = 1$;
Set $select\_num = 1$;
if $mov\_flag == 1$ **then**
    Wait for 2 seconds ;
    Set $mov\_flag = 0$;
    Set $select\_count = 0$;
    while $mov\_flag == 0$ *or* $initialize\_flag == 1$ **do**
        Sort the data groups (1-6) in descending order of (E_1, E_2, ..., E_6);
        if *New first group index equals to the former first group index* **then**
            $select\_count++$;
            if $select\_count == 3$ **then**
                Choose the first data group;
                Set $initialize\_flag = 0$;
                Set $select\_count = 0$;
                Break ;
            end
        end
        else
            Set $select\_count = 0$;
        end
    end
end
Return the index of the most sensitive data group ;

local energy of the CSI data groups (i.e., E_1, E_2, ..., E_6). If a group is ranked top 1 for three consecutive times, it will be selected as the most sensitive data group. If the top-ranked group is changed before the $select\_count$ reaches 3, the counting number will be reset to zero. Moreover, if there is a new movement detected, the signal selection will be restarted. ResBeat can keep on using the previously selected data group to monitor breathing beats until the next most sensitive data group is selected. The proposed signal selection algorithm is robust to environment interference and small movements of the body. Moreover, with the signal selection module, ResBeat can rapidly recover for large body movements.

D. Breathing Signal Monitoring

Although both CSI amplitude and phase difference data can be used to extract the breathing signal, the most sensitive data group selected as in the previous section should be used to effectively mitigate the effect of anomalous breathing signal (as shown in Fig. 1). Traditionally, an FFT based method can estimate the breathing frequency using a larger moving window size to achieve good accuracy. However, the FFT based method is not suitable for realtime breathing rates estimation. In the proposed ResBeat system, we employ peak detection to derive the breathing rate in realtime.

For effective peak detection, we still need to deal with the fake peaks in the breathing components, which is not a true peak but its value is larger than two neighboring data points. To avoid fake peaks, we employ a moving window approach with a window size of 13 samples, to identify all the true peaks in a buffer with 100 data points. A peak is detected by determining whether the middle one (i.e., the seventh point) of all the samples in the 13-sample window is equal to the maximum value. Then, we can compute the breathing period p by averaging all peak-to-peak intervals. Because the buffered data will be updated in realtime, we use a small buffer of 20 data points to store the 20 estimated breathing periodic values. Then, the final period of the breathing signal is computed by $P = \frac{1}{20}\sum_{i=1}^{i=20} p_i$. Finally, we obtain an estimated breathing rate as $60/P$ bpm.

IV. Experimental Study

A. Experiment Setting

In our experiments, ResBeat operates in the 5GHz ISM band. Our ResBeat system is executed on the Ubuntu Desktop 14.04 LTS OS for both the transmitter and receiver, each of which is equipped with an Intel 5300 NIC. The transmitter is a Lenovo laptop set in the injection model, which transmits 10 packets per second using one antenna. The receiver is an Acer laptop working in the monitoring mode for collecting CSI data, where the three antennas are placed in a row with an interval of 2.68 cm. The ResBeat system collects realtime CSI amplitude and phase difference data from the three antennas for breathing beats monitoring.

We test the proposed Resbeat system in three different indoor environments as shown in Fig. 4. In the first environment, both the transmitter and receiver are placed in a laboratory with an area of 4.5 $\times$ 8.8 m^2; the person stays at an arbitrary location in the laboratory. The second case is a through-wall scenario to test the performance of the ResBeat system when the received signal is weak. The third scenario is a long corridor to examine the influence of long distances between the transmitter and receiver. Omnidirectional antennas are used at the transmitter and receiver in all the three scenarios. In addition, the NEULOG Respiration Monitor Belt Logger Sensor is used to measure the ground truth.

As discussed in Section II-B, the breathing signal could be extremely weak at certain measurement locations, which is hard to detect [16]. To measure the resilience of breathing rate monitoring methods, we define a *success rate* performance metric, denoted by η, as

$$\eta = \frac{1}{N}\sum_{i=1}^{N}\left(\frac{\text{sgn}(2-e_i)+1}{2}\right), \tag{8}$$

where e_i is the breathing estimation error in bpm for the i_{th} location, sgn$(\cdot)$ is the `sign` function, and N is the total number of different locations tested in the experiment. The success rate represents the ratio of the number of locations having an error less than 2 bpm to the total number of locations.

B. Performance of Breathing Rate Estimation

Fig. 5 plots the cumulative distribution functions (CDF) of estimation errors of breathing rate in the computer laboratory,

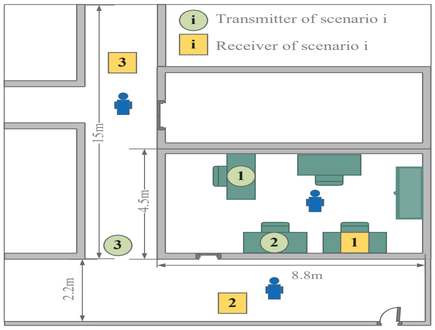

Fig. 4. Configuration of the ResBeat experiments.

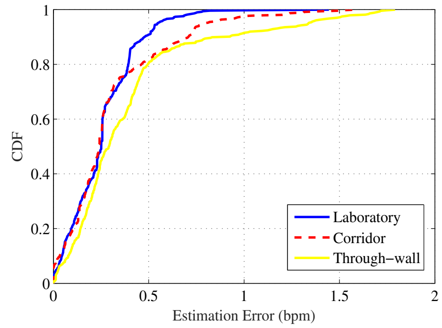

Fig. 5. Performance of breathing rate estimation.

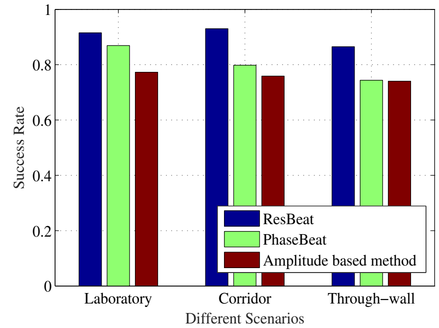

Fig. 6. Success rates of three different schemes.

through-wall, and long corridor scenarios. We find that ResBeat achieves lower breathing beats estimation errors, where the maximum error is less than 1.75 bpm. Moreover, it can be seen that for ResBeat, the median errors are 0.25 bpm, 0.25 bpm, and 0.3 bpm for the computer laboratory, long corridor, and through-wall cases, respectively. The breathing estimation errors in the laboratory and long corridor scenarios are lower than that in the through-wall scenario. This is because the breathing signal in the through-wall scenario is much weaker. In fact, the accuracy for the through-wall scenario is still high and acceptable. We conclude that the proposed ResBeat system is robust in different scenarios.

Fig. 6 presents the success rates for three different schemes in the computer laboratory, through-wall, and long corridor scenarios. In this experiment, We use the amplitude based method [13] and PhaseBeat [14] as benchmarks for success rate comparison. We find that the proposed ResBeat system achieves high success rates about 90% in the laboratory and long corridor scenarios, and about 86% in the through-wall scenario. This means that stronger breathing signals can help to achieve higher breathing beat estimation accuracy. On the other hand, the success rate of the proposed ResBeat is higher than that of the other two schemes in all the three environments. This is because ResBeat employs bimodal CSI data and the adaptive signal selection method to select the most sensitive data group, which can effectively mitigate the effect of anomalous breathing signals at certain locations.

V. Conclusions

In this paper, we proposed ResBeat, a resilient breathing beats monitoring system using realtime bimodal CSI amplitude and phase difference data. We first presented an analysis of CSI data, which motivated the bimodal ResBeat system design. We implemented ResBeat with commodity 5GHz WiFi devices, and carried out extensive experimental studies under three indoor environments. The experimental results validated the effectiveness of the proposed ResBeat system.

Acknowledgment

This work is supported in part by the US NSF under Grant CNS-1702957, and through the Wireless Engineering Research and Education Center at Auburn University.

References

[1] O. Boric-Lubeke and V. Lubecke, "Wireless house calls: Using communications technology for health care and monitoring," *IEEE Microwave Mag.*, vol. 3, no. 3, pp. 43–48, Apr. 2002.

[2] C. Hunt and F. Hauck, "Sudden infant death syndrome," *Can. Med. Assoc. J*, vol. 174, no. 13, pp. 1309–1310, Apr. 2006.

[3] M. L. R. Mogue and B. Rantala, "Capnometers," *Journal of clinical monitoring*, vol. 4, no. 2, pp. 115–121, Apr. 1988.

[4] X. Wang, R. Huang, and S. Mao, "SonarBeat: Sonar phase for breathing beat monitoring with smartphones," in *Proc. IEEE ICCCN 2017*, Vancouver, Canada, July/Aug. 2017, pp. 1–8.

[5] ——, "Demo abstract: Sonarbeat: Sonar phase for breathing beat monitoring with smartphones," in *Proc. IEEE SECON 2017*, San Diego, CA, June 2017, pp. 1–2.

[6] F. Adib, H. Mao, Z. Kabelac, D. Katabi, and R. Miller, "Smart homes that monitor breathing and heart rate," in *Proc. ACM CHI'15*, Seoul, Korea, April 2015, pp. 837–846.

[7] Z. Yang, P. Pathak, Y. Zeng, X. Liran, and P. Mohapatra, "Monitoring vital signs using millimeter wave," in *Proc. IEEE MobiHoc'16*, Paderborn, Germany, July 2016, pp. 211–220.

[8] P. Nguyen, X. Zhang, A. Halbower, and T. Vu, "Continuous and fine-grained breathing volume monitoring from afar using wireless signals," in *Proc. IEEE INFOCOM'16*, San Francisco, CA, Apr. 2016, pp. 1–9.

[9] J. Salmi and A. F. Molisch, "Propagation parameter estimation, modeling and measurements for ultrawideband MIMO radar," *IEEE Trans. Microw. Theory Technol.*, vol. 59, no. 11, pp. 4257–4267, Nov. 2011.

[10] H. Abdelnasser, K. A. Harras, and M. Youssef, "Ubibreathe: A ubiquitous non-invasive WiFi-based breathing estimator," in *Proc. IEEE MobiHoc'15*, Hangzhou, China, June 2015, pp. 277–286.

[11] D. Halperin., W. J. Hu., A. Sheth., and D. Wetherall., "Predictable 802.11 packet delivery from wireless channel measurements," in *Proc. ACM SIGCOMM'10*, New Delhi, India, Sept. 2010, pp. 159–170.

[12] Y. Xie, Z. Li, and M. Li, "Precise power delay profiling with commodity WiFi," in *Proc. ACM Mobicom'15*, Paris, France, Sept. 2015, pp. 53–64.

[13] J. Liu, Y. Wang, Y. Chen, J. Yang, X. Chen, and J. Cheng, "Tracking vital signs during sleep leveraging off-the-shelf WiFi," in *Proc. ACM Mobihoc'15*, Hangzhou, China, June 2015, pp. 267–276.

[14] X. Wang, C. Yang, and S. Mao, "PhaseBeat: Exploiting CSI phase data for vital sign monitoring with commodity WiFi devices," in *Proc. IEEE ICDCS 2017*, Atlanta, GA, June 2017, pp. 1230–1239.

[15] ——, "Tensorbeat: Tensor decomposition for monitoring multi-person breathing beats with commodity WiFi," *ACM Transactions on Intelligent Systems and Technology*, to appear.

[16] H. Wang, D. Zhang, J. Ma, Y. Wang, Y. Wang, D. Wu, T. Gu, and B. Xie, "Human respiration detection with commodity WiFi devices: Do user location and body orientation matter?" in *Proc. ACM Ubicomp'16*, Heidelberg, Germany, Sept. 2016, pp. 25–36.

[17] Z. Yang, Z. Zhou, and Y. Liu, "From RSSI to CSI: Indoor localization via channel response," *ACM Computing Surveys*, vol. 46, no. 2, pp. 25:1–25:32, Nov. 2013.

[18] W. Wang, A. X. Liu, M. Shahzad, K. Ling, and S. Lu, "Understanding and modeling of WiFi signal based human activity recognition," in *Proc. ACM Mobicom'15*, Paris, France, Sept. 2015, pp. 65–76.

[19] J. Gjengset, J. Xiong, G. McPhillips, and K. Jamieson, "Phaser: Enabling phased array signal processing on commodity WiFi access points," in *Proc. ACM Mobicom'14*, Maui, HI, Sept. 2014, pp. 153–164.

[20] S. Roberts, "Control chart tests based on geometric moving averages," *Technometrics*, vol. 42, no. 1, pp. 97–101, Feb. 2000.